Tribology International 59 (2013) 121–128

Contents lists available at SciVerse ScienceDirect

Tribology International

journal homepage: www.elsevier.com/locate/triboint

Friction torque of cylindrical roller thrust bearings lubricated with wind turbine gear oils

Carlos M.C.G. Fernandes [a,*], Ramiro C. Martins [a], Jorge H.O. Seabra [b]

[a] INEGI, Universidade do Porto, Campus FEUP, Rua Dr. Roberto Frias 400, 4200-465 Porto, Portugal
[b] FEUP, Universidade do Porto, Rua Dr. Roberto Frias s/n, 4200-465 Porto, Portugal

ARTICLE INFO

Article history:
Received 2 August 2011
Received in revised form
17 April 2012
Accepted 22 May 2012
Available online 15 June 2012

Keywords:
Gear oils
Rolling bearings
Friction torque
Efficiency

ABSTRACT

Planetary gearboxes used in wind turbines very often have premature bearing and gear failures, some of them related to the lubricants used. Five fully formulated windmill gear oils with the same viscosity grade and different formulations were selected and characterized. The lubricant tribological behavior in a cylindrical roller thrust bearing was analyzed. A modified four-ball machine was used to assemble the bearings. They were submitted to an axial load and the tests were performed at velocities ranging between 150 and 1500 rpm. Experimental results for the operating temperatures and for the internal friction torque are presented.

© 2012 Elsevier Ltd. All rights reserved.

1. Introduction

As proven source of clean and affordable energy, wind resources clearly have a vital role to play in energetic sustainability [1]. In this sense it is necessary to have wind turbines that maximize the use of eolic energy and achieve their design life goals with minimal maintenance.

Gearboxes have plagued the wind power industry [2]. Wind turbine failures can be extremely costly in terms of repair costs, replacement parts and lost power, and the gearbox is the most likely component to have a major effect on the turbine availability. Since the establishment of the wind energy industry large failure rates of the gearboxes have been observed. Windmills, often placed in hostile environments, have premature bearing and gear failures, and the performance of the gear oils used for their lubrication also have an important role in gearbox reliability. Most wind turbine gearbox failures are rooted to the bearings [3].

Due to economic and environmental constraints it is mandatory to increase the efficiency of windmills, to reach the highest efficiency of planetary gear drives and their parts (gears, rolling bearings, seals, etc.) and to minimize the heat generation in the gearboxes [4]. In order to increase gearbox efficiency it is important identify the main sources of power loss. The most common wind turbine gearboxes have planetary gears and the main losses occurring are: friction loss between the meshing teeth [5–10], friction loss in the bearings [5,11,12], friction loss in the seals [5], lubricant churning losses [13,14] and energy loss due to air-drag [4].

Friction generated between the meshing teeth is the main source of power loss in a planetary gear. On the other hand, rolling bearing friction is also very important because it can reach about 30% of total power loss occurring within the mechanism [15]. In this sense, understand the friction torque generated within rolling bearings is essential in order to reduce their contribution to the overall power loss. There are four physical friction sources inside a rolling bearing: rolling friction [16], sliding friction, seal friction and drag losses [17]. The most important ones in the case of windmill applications (high torque and low speed) are the friction occurring in the contact between the rolling elements and raceways (sliding friction) and the friction due to the lubricant flow between the bearing elements (rolling friction). These energy loss mechanisms are highly dependent on the lubricant ability to generate an effective oil film between the rolling elements and the raceways and on the physical properties of the gear oils.

Wind turbine gearboxes are composed of various mechanical parts, including different types of rolling bearings [18]. In this sense we intend to identify the loss mechanisms occurring in rolling bearings lubricated with wind turbine gear oils. For that purpose the friction torque losses in cylindrical roller thrust bearings (81107) were identified and compared when different lubricants are used. Five different fully formulated gear oils were characterized and tested on a cylindrical roller thrust bearing (81107) submitted to an axial load of 7000 N and rotational speeds between 150 and 1500 rpm. The tests were performed on a modified four-ball machine (Cameron-Plint TE 82/7752) using a special assembly for the thrust roller bearings (81107).

* Corresponding author. Tel.: + 351 225082212.
E-mail address: cfernandes@inegi.up.pt (C.M.C.G. Fernandes).

0301-679X/$ - see front matter © 2012 Elsevier Ltd. All rights reserved.
http://dx.doi.org/10.1016/j.triboint.2012.05.030

2. Lubricant physical properties

All the lubricants tested are fully formulated gear oils have a viscosity grade ISO VG 320 and may be used in the lubrication of wind turbine gearboxes. This is a comparative study of different base oils: ester (ESTF and ESTR), mineral (MINR), polyalkyleneglycol (PAGD) and polyalphaolefin (PAOR). Table 1 displays the physical properties of the five lubricants as well as their chemical composition.

2.1. Chemical composition

Using the ICP method according to ASTM D 5185, the chemical composition of the lubricants was determined and presented in Table 1. The elements identified were zinc (Zn), magnesium (Mg), phosphorus (P), calcium (Ca) and boron (B). It is clear that the formulations are significantly different, both in terms of base oil and additive package.

2.2. Density

The densities of the gear oils at 15 °C, provided by the lubricant manufacturers, are presented in Table 1. The gear oil densities were also measured at 40, 70 and 100 °C using a *DMA* 35*N* densimeter. The values measured were used to calculate the thermal expansion coefficient α_t of the gear oils, according to Eq. (1). The results are presented in Table 1

$$\rho = \rho_0 + \alpha_t \cdot \rho_0 (T - T_{ref}) \quad (1)$$

2.3. Kinematic viscosity

The kinematic viscosities of each oil were measured using an Engler viscometer. The measurements were performed at 40, 70 and 100 °C according to ASTM D341 and are displayed in Table 1. At 40 °C all the kinematic viscosities were very similar, since all the gear oils had the same viscosity grade. However, at 100 °C the kinematic viscosities were significantly different: 22.3 cSt for the MINR oil, 51.6 cSt for the PAGD and 33.3, 34.9 and 36.6 for the PAOR, ESTR and ESTF, respectively.

The kinematic viscosities were used to determine the Viscosity Index of each lubricant. The MINR gear oil had the lowest VI (85) while the PAGD oil had the highest value (241). The PAOR, ESTR, ESTF gear oils had intermediate values, respectively, 153, 162 and 159.

2.4. Dynamic viscosity

The dynamic viscosities of the oils were also measured using a Contraves Rheomat 115 rheometer with a rotary viscometer with coaxial cylinders. The measurements were performed at 40, 70 and 100 °C, and several shear strain rates (6.387, 26.786, 112.477, 472.479 and 967.280). The results are displayed in Fig. 1. The corresponding kinematic viscosities are presented in Fig. 2.

At 40 °C the dynamic viscosity was not independent of the shear strain rate, indicating that the lubricant behavior was

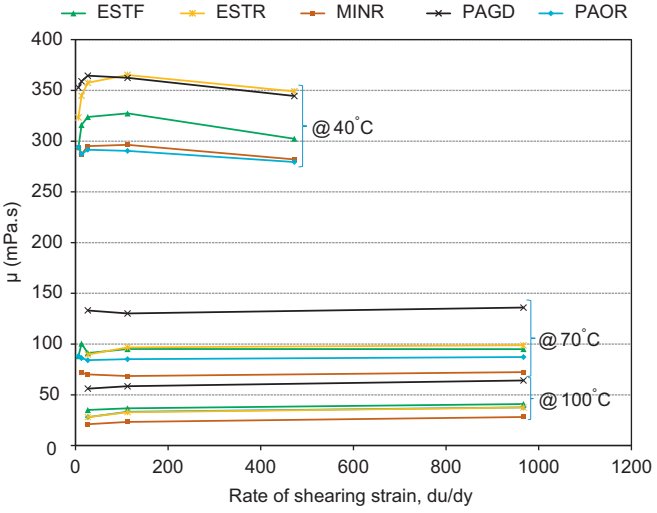

Fig. 1. Dynamic viscosity vs. shear strain rate.

Table 1
Physical properties of lubricants used.

Parameter	Unit	ESTF	ESTR	MINR	PAGD	PAOR
Base oil	(–)	Ester	Ester	Mineral	Polyalkyleneglycol	Polialphaolefin
Chemical composition						
Zinc (Zn)	(ppm)	0.7	6.6	0.9	1	3.5
Magnesium (Mg)	(ppm)	1.3	1.3	0.9	1.4	0.5
Phosphorus (P)	(ppm)	449.4	226.2	354.3	1100	415.9
Calcium (Ca)	(ppm)	n.d.	14.4	2.5	0.8	0.5
Boron (B)	(ppm)	33.6	1.7	22.3	1.0	28.4
Sulfur (S)	(ppm)	5030	406	11 200	362	5020
Physical properties						
Density, 15 °C	(g/cm^3)	0.957	0.915	0.902	1.059	0.859
Thermal expansion coefficient (α_t)	(/)	-6.7×10^{-4}	-8.1×10^{-4}	-5.8×10^{-4}	-7.1×10^{-4}	-5.5×10^{-4}
Viscosity, 40 °C	(cSt)	324.02	302.86	319.22	290.26	313.52
Viscosity, 70 °C	(cSt)	88.09	77.48	65.87	102.33	84.99
Viscosity, 100 °C	(cSt)	36.06	34.85	22.33	51.06	33.33
m	(/)	2.695	2.682	3.459	2.752	2.049
n	(/)	7.126	7.088	9.031	7.266	5.505
Thermoviscosity, 40 °C ($\beta\times10^{-3}$)	($°K^{-1}$)	49.90	49.09	63.88	37.34	50.68
Thermoviscosity, 70 °C ($\beta\times10^{-3}$)	($°K^{-1}$)	35.78	35.25	42.83	28.36	36.16
Thermoviscosity, 100 °C ($\beta\times10^{-3}$)	($°K^{-1}$)	26.55	26.19	30.07	22.12	26.72
s, 0.2 GPa	(/)	6.605	6.605	9.904	5.489	7.382
t, 0.2 GPa	(/)	0.136	0.136	0.139	0.149	0.134
Piezoviscosity, 40 °C ($\alpha\times10^{-8}$)	(Pa^{-1})	1.450	1.437	2.207	1.278	1.590
Piezoviscosity, 70 °C ($\alpha\times10^{-8}$)	(Pa^{-1})	1.220	1.212	1.774	1.105	1.339
Piezoviscosity, 100 °C ($\alpha\times10^{-8}$)	(Pa^{-1})	1.076	1.071	1.527	0.988	1.182
VI	(/)	159	162	85	241	153

non-Newtonian. At higher temperatures (70 and 100 °C) such non-Newtonian behavior was no longer observed and the dynamic viscosity was constant whatever the shear strain rate. This behavior was observed for all the gear oils.

2.5. Thermoviscosity

The kinematic viscosities were used to determine the thermoviscosity of the oils, using the following equation:

$$\beta = \frac{m}{T}\frac{(\upsilon+a)\ln(\upsilon+a)}{\upsilon} \quad (2)$$

The constants m and n (ASTM D341) as well as the thermoviscosity values calculated for each oil are presented in Table 1. The constant a is 0.7 cSt according to the standard. The thermoviscosity values follow the inverse trend of the Viscosity Index (high Viscosity Index implies a low thermoviscosity value).

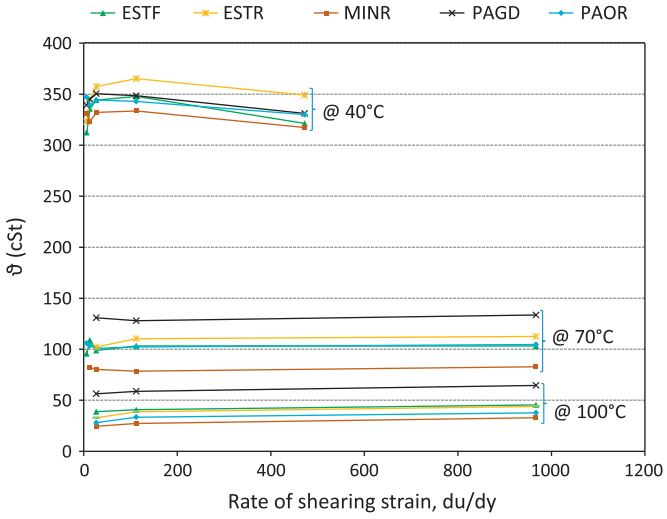

Fig. 2. Kinematic viscosity vs. shear strain rate.

2.6. Piezoviscosity

Gold et al. [19] proposed Eq. (3) to calculate the piezoviscosity of oils formulated with different base oils

$$\alpha = sv^t \quad (3)$$

The constants s and t as well as the piezoviscosity values calculated for each oil are presented in Table 1. The MINR gear oil had the highest piezoviscosity (17.3×10^{-9} GPa^{-1}) while the PAGD oil had the lowest value (8.9×10^{-9} GPa^{-1}). The PAOR, ESTR, ESTF gear oils had intermediate values, respectively, 12.9×10^{-9} GPa^{-1}, 11.3×10^{-9} GPa^{-1} and 10.9×10^{-9} GPa^{-1}.

The piezoviscosity has a very significant influence on lubricant film thickness between roller and raceways in a cylindrical roller thrust bearing.

3. Rolling bearing assembly and test procedures

The rolling bearing tests were performed on a modified four-ball machine, where the four-ball arrangement was replaced by a rolling bearing assembly, as shown in Fig. 3. This assembly was developed to test several rolling bearings and measure the friction torque and the operating temperature in several different points. A detailed presentation of this assembly can be found in [20].

The rolling bearing assembly is divided in two parts: the shaft adapter (6), directly connected to the machine shaft and supporting the bearing upper race (5); a lower race support (2) and the bearing lower race (3), both clamped to the bearing housing (1). In operation, the internal bearing torque (or friction torque) is transmitted to the torque cell (11) through the bearing housing (1). The friction torque was measured with a piezoelectric torque cell *KISTLER*9339*A*, ensuring high-accuracy measurements even when the friction torque generated in the bearing was very small compared to the measurement range available.

This assembly has five thermocouples (I–V), measuring temperatures at strategic locations (see Fig. 3) which are used to monitor the temperature inside the bearing assembly (IV), near to

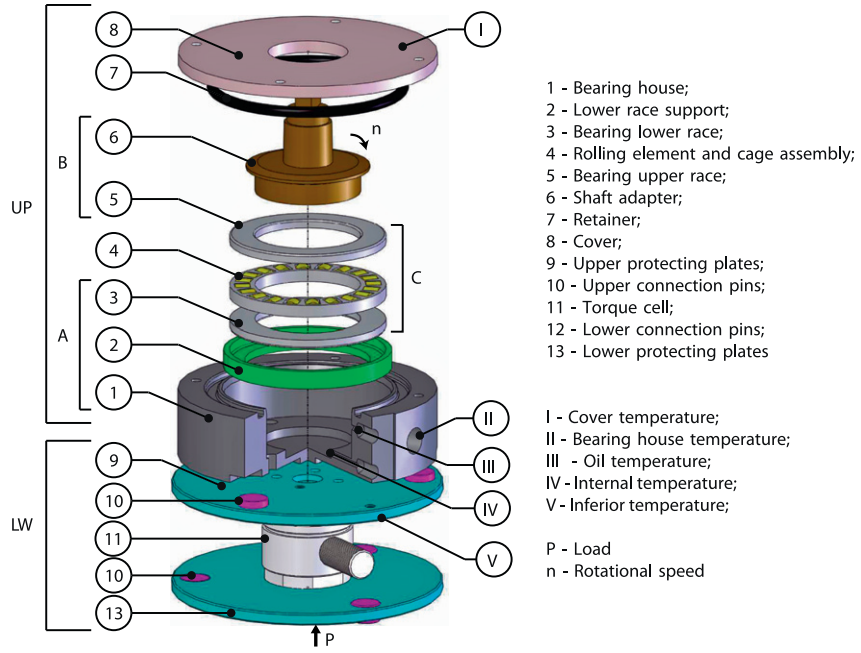

Fig. 3. Schematic view of the rolling bearing assembly.

the rolling bearing and the lubricant (III) and to evaluate the heat evacuation from the bearing housing into the surrounding environment (I, II and V). The system is also monitored by two thermocouples to quantify the chamber and room temperatures.

When assembled in the modified four-ball machine the rolling bearing assembly is submitted to a continuous air flow, forced by two 38 mm diameter fans running at 2000 rpm, cooling the chamber surrounding the bearing house.

The rolling bearing is lubricated by an oil volume of 14 ml. This volume was selected so that the oil level reaches the center of the roller, such as advised by the manufacturer.

3.1. Start-up friction torque procedure

After mounting the rolling bearing assembly and connecting the thermocouples and the torque cell, a static axial load of 7000 N was applied. The rolling bearing monitoring system [20] and the four-ball machine were turned on and the speed was increased from rest to 150 rpm in 60 s, at room temperature, while the bearing friction torque is monitored. The starting friction torque is the maximum friction torque recorded during this period.

3.2. Total friction torque procedure

All roller thrust bearing tests were performed applying an axial load of 7000 N and rotation speeds in the range 150–1500 rpm. A detailed presentation of the test procedure can be found in [20].

The machine was started at the desirable speed and run until it reached a constant temperature. Under these conditions, four friction torque measurements were performed: three values are stored and the most dispersed one was disregarded. Due to the "drift effect" which affects the measurements of the piezoelectric sensors after long periods of operation, the friction torque measurements should be made in a short period of time (less than 120 s) and at constant temperature (± 2 °C).

4. Experimental results

4.1. Start-up friction torque

The start-up friction torque is the minimum torque necessary for the rolling bearing to start rotating from rest. The measurements were performed in the same conditions for all gear oils, at almost the same operating temperature, see Table 2.

The start-up friction torques of the roller thrust bearings (RTB's) lubricated with each oil are presented in Table 2: the PAGD oil generated the highest RTB start-up friction torque, followed by MINR and PAOR. ESTF and ESTR oils generated significantly lower RTB start-up friction torque than other formulations.

4.2. Operating and stabilization temperatures

The operating temperature is the one measured in the thermocouple (III), as shown in Fig. 3. The operating temperature of the RTB increases when the operating speed increases, whatever the gear oil considered, as shown in Fig. 4. At 150 rpm the operating temperatures of the RTB lubricated were very similar, between 33.9 °C for ESTF gear oil and 35.9 °C for MINR oil. At 1500 rpm the operating temperatures of the RTB were significantly higher: $\theta^{PAOR} = 87.0$ °C, $\theta^{ESTR} = \theta^{ESTF} = 92.3$ °C, $\theta^{PAGD} = 100.0$ °C and $\theta^{MINR} = 107$ °C.

The stabilization temperatures of the RTB, defined as the difference between the operating and chamber temperatures, that is, $\theta_s = \theta - \theta_c$, are presented in Fig. 5. As in the case of the operating temperature, the stabilization temperature of the RTB increased when the operating speed increased. The RTB lubricated with the MINR gear oil always had the highest stabilization temperature, followed by the RTB lubricated with the PAGD oil. The RTBs lubricated with the PAOR, ESTR and ESTF oils had very similar stabilization temperatures, lower than those obtained for MINR and PAGD oils. At 1500 rpm the following RTB stabilization temperatures were measured: $\theta_s^{MINR} = 68.3$ °C, $\theta_s^{PAGD} = 63.0$ °C, $\theta_s^{ESTF} = 55.8$ °C, $\theta_s^{ESTR} = 54.4$ °C and $\theta_s^{PAOR} = 48.6$ °C.

These results clearly show that gear oil formulation had a very significant influence on the stabilization temperatures of the 81107 RTB.

4.3. Friction torque and power loss

The internal friction torque of the RTB, measured at different rotating speeds (150–1500 rpm) and for each gear oil tested is plotted in Fig. 6. As expected, the friction torque inside the RTB decreased when the operating speed increased whatever the gear oil considered.

Table 2
Operating temperature, kinematic viscosity and start-up friction torque at 150 rpm.

Base oil	ESTF	ESTR	MINR	PAGD	PAOR
Operating temperature (°C)	26.6	27.0	25.6	28.6	25.5
Kinematic viscosity (mm^2/s)	579.39	635.11	891.06	463.50	707.42
Start-up friction torque (N mm)	448	470	648	673	577

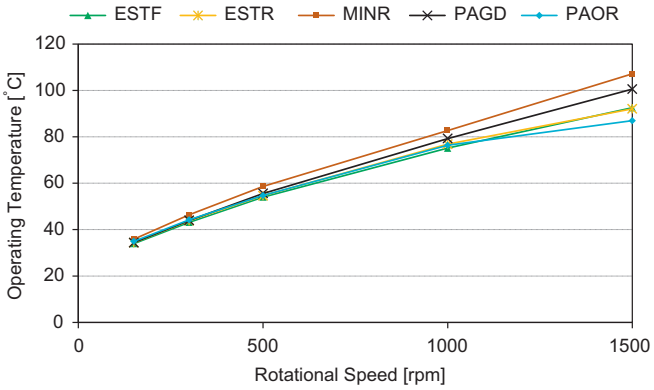

Fig. 4. Operating temperature vs. rotational speed.

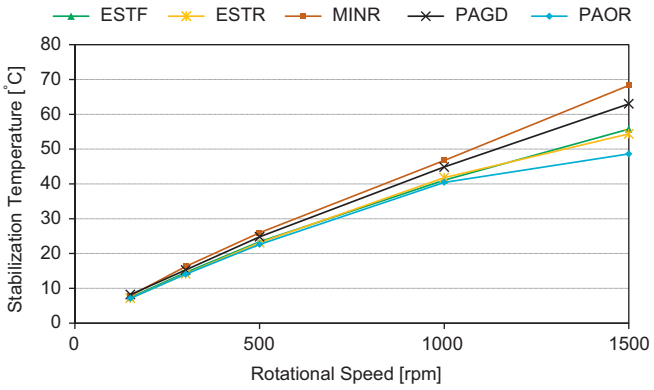

Fig. 5. Stabilization temperature vs. rotational speed.

The RTB lubricated with MINR oil always generated the highest friction torque followed closely by the RTB lubricated with PAGD oil. The RTB lubricated with ESTF oil always had the lowest friction torque. Depending on the operating speed, the friction torques generated by RTB's lubricated with ESTF and PAOR oils were close either to the MINR and PAGD oils (higher values) or to the ESTF oil (lower values).

Knowing the internal friction torque and the operating speed it is possible to calculate the power loss (ΔP) in the RTB, using the following equation:

$$\Delta P = M_{exp} \cdot \omega \tag{4}$$

The power loss results are plotted in Fig. 7. The power loss increased when the operating speed increased, reaching a maximum of 48–52 W at 1500 rpm, depending on the gear oil considered. The RTB lubricated with the MINR oil always had the highest power loss and the RTB lubricated with ESTF the lowest one.

5. Film thickness in the roller–raceway contact

The center film thickness in the roller–raceway contact can be determined by using Eqs. (5)–(8) for line or rectangular contacts, derived by Dowson and Higginson [21]. The geometry of the roller–raceway contact in the RTB was used as well as the oil properties at the corresponding operating temperatures

$$H_0 = 1325 \cdot R_x \cdot U^{0,70} \cdot G^{0,54} \cdot W^{-0,13} \cdot C_0 \tag{5}$$

$$U = \frac{\eta_0 (U_1 + U_2)}{2 R_X E^*} \tag{6}$$

$$G = 2\alpha E^* \tag{7}$$

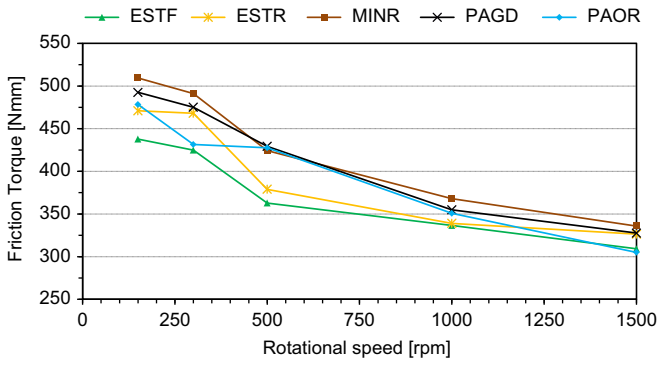

Fig. 6. Friction torque vs. rotational speed.

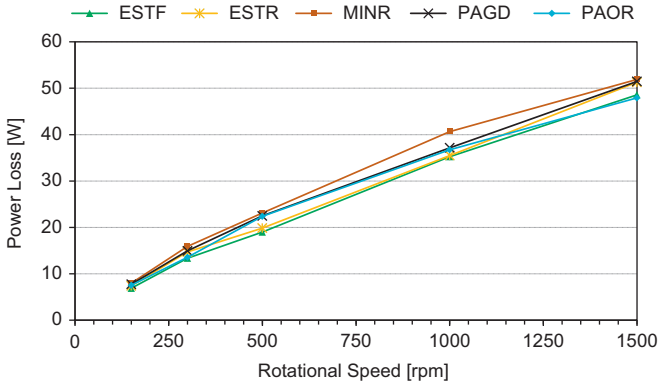

Fig. 7. Power loss vs. rotational speed.

$$W = \frac{F_n}{R_X l E^*} \tag{8}$$

The theoretical film thickness h_0 was corrected using the thermal reduction factor (ϕ_T) due to inlet shear heating, as shown in Eqs. (9)–(12). The specific film thickness was computed with Eq. (13), taking into account the composite roughness of the roller thrust bearing ($\sigma = 0.14$ μm). Several measurements of the roller and raceways surface roughness were made with an absolute stylus probe (measuring length 4.8 mm, cut-off 0.8 mm).

Knowing the specific film thickness in the roller–raceway contact, it is possible to evaluate the corresponding lubrication regime

$$h_{0C} = \phi_T \cdot H_0 \tag{9}$$

$$\phi_T = \{1 + 0.1(1 + 14.8 S^{0.83}) L^{0.64}\}^{-1} \tag{10}$$

$$L = \frac{\beta \eta_0 (U_1 + U_2)^2)}{K} \tag{11}$$

$$S = \frac{|U_1 - U_2|}{U_1 + U_2} \tag{12}$$

$$\Lambda = \frac{h_{0C}}{\sqrt{\sigma_1^2 + \sigma_2^2}} \tag{13}$$

Fig. 9 shows the evolution of specific film thickness in the roller–raceway contact with the rotational speed. Gear oils ESTF, ESTR and PAOR had a similar behavior for all the speed ranges, reaching the maximum specific film thickness at 300 rpm. The specific film thickness calculated for the ESTF gear oil was in the range 1.25–1.80, typical of mixed film lubrication.

PAOR gear oil had a slightly different behavior, generating the highest specific film thickness of all oils at 500 rpm and above that speed. This different behavior of the PAGD gear oil is explained by its very high Viscosity Index (241), meaning that its viscosity drops significantly less than the other lubricants when the operating speed and temperature of the RTB increased (see Fig. 8), although it had the lowest pressure–viscosity coefficient (see Table 1).

The MINR gear oil had the opposite behavior of the PAGD oil, generating the lowest specific film thickness of all oils above 500 rpm. This behavior of the MINR oil is explained by its low Viscosity Index (85), meaning that its viscosity drops significantly more than the other lubricants when the operating speed and temperature of the RTB increased (see Fig. 8), although it had the highest pressure–viscosity coefficient (see Table 1). Fig. 9 also shows that RTB lubricated with the MINR gear oil operated in boundary film lubrication at 1500 rpm, since its specific film thickness was below 1.0 at that speed.

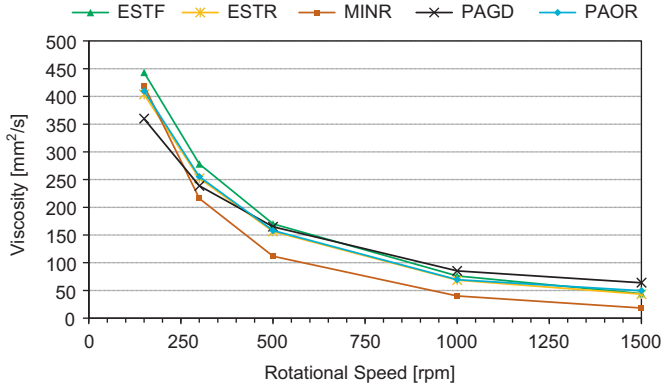

Fig. 8. Kinematic viscosity vs. rotational speed.

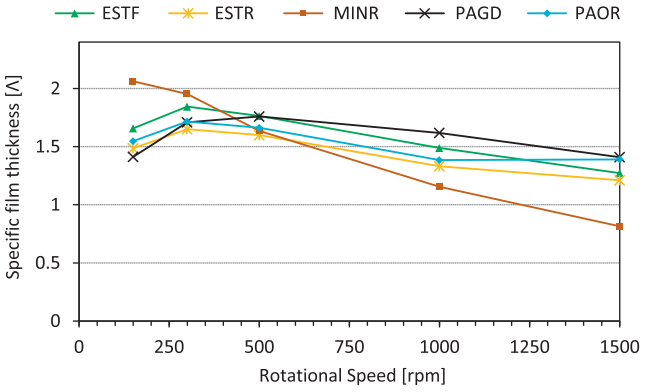

Fig. 9. Specific film thickness vs. rotational speed.

6. Friction torque model and discussion

In order to understand the friction torque behavior of the RTB lubricated with each gear oil, a friction torque model is needed to quantify the different components of the friction torque. The friction torque model proposed by SKF [12] was used.

The model considers that the total friction torque is the sum of four different physical sources of torque loss, represented by the following equation:

$$M_t = M'_{rr} + M_{sl} + M_{drag} + M_{seal} \tag{14}$$

The cylindrical roller thrust bearing (81107) does not have seals and so the M_{seal} torque loss term was disregarded. The drag losses were very small because the operating speeds and the mean diameter of the RTB are small and, consequently, the drag torque loss term was also disregarded. Thus, the total friction torque of the roller thrust bearing had only two terms: the rolling and sliding torques, respectively, M'_{rr} and M_{sl}, as represented by the following equation:

$$M_{exp} = M_t = M'_{rr} + M_{sl} \tag{15}$$

Since the total friction torque was measured experimentally ($M_t = M_{exp}$), it was possible to calculate the sliding torque once the rolling torque was known

$$M_{sl} = M_t - M'_{rr} = M_{exp} - M'_{rr} \tag{16}$$

Eqs. (17)–(24) define the rolling and sliding torques

$$M'_{rr} = \phi_{ish} \cdot \phi_{rs} [G_{rr} (n \cdot \upsilon)^{0.6}] \tag{17}$$

$$\phi_{ish} = \frac{1}{1 + 1.84 \times 10^{-9} (n d_m)^{1.28} \nu^{0.64}} \tag{18}$$

$$\phi_{rs} = \frac{1}{e^{K_{rs} \nu n (d+D) \sqrt{\frac{K_z}{2(D-d)}}}} \tag{19}$$

$$G_{rr} = R_1 \cdot d_m^{2.38} \cdot F_a^{0.31} \tag{20}$$

$$M_{sl} = G_{sl} \cdot \mu_{sl} \tag{21}$$

$$G_{sl} = S_1 \cdot d_m^{0.62} \cdot F_a \tag{22}$$

$$\mu_{sl} = \phi_{bl} \cdot \mu_{bl} + (1 - \phi_{bl}) \cdot \mu_{EHD} \tag{23}$$

$$\phi_{bl} = \frac{1}{e^{2.6 \times 10^{-8} (n \cdot \upsilon)^{1.4} d_m}} \tag{24}$$

The constants S_1 and R_1 for RTB are equal to 0.154 and 2.25×10^{-6}, respectively.

The rolling torque (Eq. (17)) is mainly influenced by the viscosity of the gear oil, at the operating temperature, and by the rotational speed ($(n \cdot \upsilon)^{0.6}$). The product of the "kinematic replenishment factor" by the "inlet shear heating factor" ($\phi_{rs} \cdot \phi_{ish}$) decreases when the operating speed increases.

The sliding torque is highly affected by the load weighting factor and by the coefficient of friction in full film EHD lubrication, ϕ_{bl} and μ_{EHD}, respectively. The load weighting factor ϕ_{bl} increases when the specific film thickness decreases and this affects the sliding coefficient of friction, μ_{sl}, and the sliding torque.

6.1. Rolling friction torque

The rolling friction torque M'_{rr} inside the roller thrust bearing was determined using Eqs. (17)–(20) and the operating temperatures measured during the RTB tests. The results obtained are shown in Fig. 10. The RTBs lubricated with synthetic gear oils (ESTF, ESTR, PAGD and PAOR) had similar rolling friction torques, in the range 175–225 N mm depending on the lubricant considered. Furthermore the values determined are not significantly influenced by the rotating speed, meaning that for these gear oils with high Viscosity Index the product $n \cdot \upsilon$, remained almost constant when the rotating speed increased. In fact, higher speed generates higher operating temperature and, consequently lower operating viscosity and $n \cdot \upsilon \cong const$.

The RTB lubricated with the MINR gear oil had a significantly different behavior, where the rolling friction torque decreased continuously while the rotating speed increased (190 N mm at 150 rpm to 116 N mm at 1500 rpm). This behavior is typical of RTB lubricated with low Viscosity Index mineral fluids.

6.2. Sliding friction torque

Since the total friction torque ($M_t = M_{exp}$) was measured and the rolling friction torque M'_{rr} was calculated, the sliding friction torque can be determined using Eq. (25), that is

$$M_{sl} = M_t - M'_{rr} = M_{exp} - M'_{rr} \tag{25}$$

Fig. 11 shows the sliding friction torque inside the RTB, at the operating speed and for each gear oil. The RTB lubricated with the MINR gear oil always had the highest sliding friction torque, 319 N mm at 150 rpm and 219 N mm at 1500 rpm. The RTBs lubricated with the synthetic gear oils generated significantly lower sliding friction torques than the MINR oil, mainly above 300 rpm. The RTB lubricated with the ESTF gear oil had significantly low sliding friction torques, 236 N mm at 150 rpm and 112 N mm at 1500 rpm, respectively, 74% and 51% of the value calculated for the RTB lubricated with the MINR oil. At 1000 and 1500 rpm the RTBs lubricated with the synthetic oils had very similar sliding friction torques.

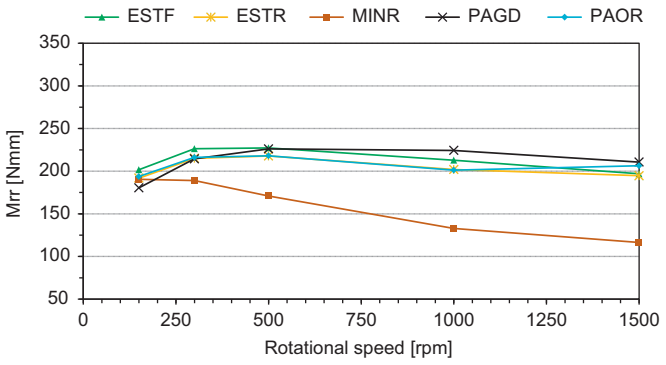

Fig. 10. Rolling torque vs. rotational speed.

6.3. Sliding coefficient of friction

Knowing the sliding friction torque, it is possible to calculate the sliding coefficient of friction corresponding to each gear oil at the operating speed, using Eqs. (26) and (22), that is

$$\mu_{sl} = \frac{M_{sl}}{G_{sl}} \tag{26}$$

The sliding coefficient of friction (sliding COF), shown in Fig. 12, follows exactly the same trend of the sliding friction torque, because G_{sl} is constant for the same RTB geometry and constant axial load (Fa=7000 N).

The high sliding coefficients of friction calculated for the RTB lubricated with MINR gear oil can be explained both by the nature of the base oil and by the operating specific film thickness calculated in that case (see Fig. 9). In fact, for the same viscosity grade and the same temperature and speed, mineral oils generate higher coefficients of friction than Ester, PAO and PAG fluids [22]. At 1000 and 1500 rpm the RTB lubricated with MINR gear oil had lower specific film thickness than the other oils ($\Lambda \cong 1$), approaching the boundary lubrication regime, justifying the high sliding coefficient of friction obtained.

At 1000 and 1500 rpm the RTBs lubricated with synthetic gear oils (ESTF, ESTR, PAOR and PAGD) had very similar sliding torques and specific film thickness (see Fig. 9) and, consequently, very similar sliding COF.

It is very interesting to analyse the sliding coefficient of friction at low speed (150 and 300 rpm). In that situation, the rolling torques of the RTB are very similar (180–200 N mm, see Fig. 10 as well as the operating temperatures and specific film thickness (1.5–2, mixed film lubrication, see Fig. 9). Consequently, the total friction torque, the sliding friction torque and the sliding COF show exactly the same trend that is, $\mu_{sl}^{MINR} > \mu_{sl}^{PAGD} > \mu_{sl}^{ESTR} > \mu_{sl}^{PAOR} < \mu_{sl}^{ESTF}$.

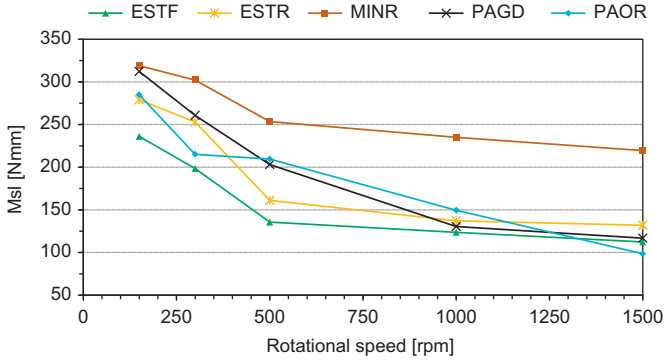

Fig. 11. Sliding torque vs. rotational speed.

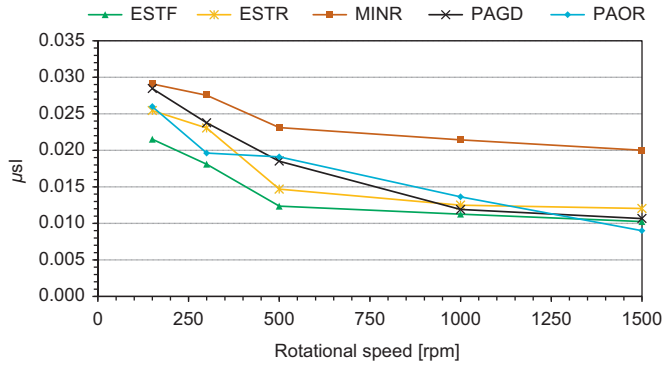

Fig. 12. Sliding coefficient of friction vs. rotational speed.

7. Conclusion

- The total friction torque inside the RTB decreased when the operating speed and temperature increased. The RTB lubricated with mineral oil had the highest friction torque and the RTB lubricated with ester oil (ESTF) had the lowest friction torque.
- The RTB's operated in mixed film lubrication ($1.25 \leq \Lambda \leq 1.80$) when lubricated with high Viscosity Index gear oils. At 1000 and 1500 rpm the RTB lubricated with mineral oil (MINR) operated close to the boundary film lubrication ($\Lambda \approx 1$).
- The RTB's lubricated with high VI gear oils had an almost constant rolling friction torque (200–225 N mm) for operating speeds equal or above 300 rpm. The rolling torque of the RTB lubricated with mineral oil decreased continuously as the operating speed increased.
- The mineral oil generated significantly higher sliding coefficient of friction than the other lubricants, mainly at 500 rpm and above. At low speed the following trend was observed: $\mu_{sl}^{MINR} > \mu_{sl}^{PAGD} > \mu_{sl}^{ESTR} > \mu_{sl}^{PAOR} > \mu_{sl}^{ESTF}$.

Notation and units

T	operating temperature (°C)
T_{ref}	reference temperature (°C)
ΔT	stabilization temperature (°C)
α_t	thermal expansion coefficient (–)
β	thermoviscosity (K^{-1})
ρ	density (g/cm^3)
ρ_0	density at reference temperature (g/cm^3)
C_0	ellipticity influence parameter (–)
d_m	bearing mean diameter (mm)
E^*	equivalent Young modulus (Pa)
Fa	axial load (N)
G	material influence parameter (–)
G_{rr}	factor that depends on the bearing type, bearing mean diameter and applied load (–)
G_{sl}	factor that depends on the bearing type, bearing mean diameter and applied load (N mm)
H_0	centered film thickness (μm)
K_{rs}	starvation constant for grease (6×10^{-8})
K_L	bearing type related geometry constant (0.43)
K_Z	bearing type related geometry constant (4.4)
L	thermal parameter of lubricant (–)
m	calculated according ASTM D341 [23] (–)
M_{exp}	bearing friction torque measured experimentally (N mm)
M_{rr}	rolling friction torque (N mm)
M_{sl}	sliding friction torque (N mm)
M_{drag}	friction torque of drag losses (N mm)
M_{seal}	friction torque of seals (N mm)
M_t	total bearing friction torque (N mm)
η	kinematic viscosity at the operating temperature (mm^2/s)
n	rotational speed (rpm)
n	calculated according ASTM D341 [23] (–)
ΔP	power loss (W)
R_1	geometry constant for rolling frictional torque (2.25×10^{-6})
S_1	geometry constant for sliding frictional torque (0.154)
s	parameter depending on lubricant package according to [19] (–)
S	sliding rate (–)

t	parameter depending on lubricant package according to [19] (–)
U	speed influence parameter (–)
U_1	linear speed of roller internal (m/s)
U_2	linear speed of roller (m/s)
VI	viscosity index (–)
W	load influence parameter (–)
ϕ_{bl}	sliding frictional torque weighting factor (–)
ϕ_{ish}	inlet shear heating reduction factor (–)
ϕ_{rs}	kinematic replenishment/starvation reduction factor (–)
ϕ_A	starvation flow reduction factor (–)
ϕ_T	thermal reduction factor (–)
ϕ_R	roughness reduction factor (–)
μ	dynamic viscosity (Pa s)
μ_{bl}	coefficient depending on the additive package in the lubricant (–)
μ_{EHD}	friction coefficient in full film conditions (–)
μ_{sl}	sliding friction coefficient (–)
Λ	specific film thickness (μm)
τ	shear stress (Pa)

Acknowledgments

The authors acknowledge to "Fundação para a Ciência e Tecnologia" for the financial support given through the project "High efficiency lubricants and gears for windmill planetary gearboxes", with research contract PTDC/EME-PME/100808/2008.

References

[1] Agency EE. Europe's onshore and offshore wind energy potential—an assessment of environmental and economic constraints. EEA technical report no. 6; 2009, 91.
[2] McNiff B, Musial W, Errichello R. Variations in gear fatigue life for different wind turbine braking strategies. In: Prepared for AWEA Wind Power '90, Washington, DC, 24–28 September 1990; 1991. Medium: ED; Size: Pages: 10.
[3] Musial W, Butterfield S, McNiff B. Improving wind turbine gearbox reliability. In: National Renewable Energy Laboratory 2007 European wind energy conference, Milan, Italy; 7–10 May 2007. p. 13.
[4] Csoban A, Kozma M. Tooth friction loss in simple planetary gears. In: Seventh international multidisciplinary conference, Baia Mare, Romania; 17–18 May 2007. p. 153–60.
[5] Höhn B-R, Michaelis K, Vollmer T, Thermal rating of gear drives: balance between power loss and heat dissipation. AGMA technical paper.
[6] Martins R, Cardoso N, Seabra J. Gear power loss performance of biodegradable low-toxicity ester-based oils. Proceedings of the Institution of Mechanical Engineers. Part J 2008;222(J3):431–40, http://dx.doi.org/10.1243/13506501jet345.
[7] Martins R, Seabra J, Brito A, Seyfert C, Luther A, Igartua R. Friction coefficient in fzg gears lubricated with industrial gear oils: biodegradable ester vs. mineral oil. Tribology International 2006;39(6):512–21, http://dx.doi.org/10.1016/j.triboint.2005.03.021.
[8] Martins R, Seabra J, Seyfert C, Luther R, Igartua A, Brito A. Power loss in fzg gears lubricated with industrial gear oils: biodegradable ester vs. mineral oil. In: Dowson D, Priest M, Dalmaz G, Lubrecht AA, editors. Tribology and interface engineering series, vol. 48. Elsevier; 2005. p. 421–30.
[9] Martins R, Moura P, Seabra J. Power loss in fzg gears: mineral oil vs. biodegradable ester and carburizedsteel vs. austempered ductile iron vs. mos2-ti coated steel, VDI Berichte 1904.2(1904 II); 2005. p. 1467–86.
[10] Magalhães L, Martins R, Locateli C, Seabra J. Influence of tooth profile and oil formulation on gear power loss. In: Tribology international, 36th Leeds–Lyon symposium, vol. 43(10); 2010. p. 1861–71. Special issue: multi-facets of tribology http://dx.doi.org/10.1016/j.triboint.2009.10.001.
[11] Eschmann P, Hasbargen L, Weigand K. Ball and roller bearings—theory, design, and application. John Wiley and Sons; 1985.
[12] SKF General Catalogue 6000 EN, SKF, November 2005.
[13] Changenet C, Velex P. A model for the prediction of churning losses in geared transmissions—preliminary results. Journal of Mechanical Design 2007;129(1):128–33, http://dx.doi.org/10.1115/1.2403727.
[14] Changenet C, Leprince G, Ville F, Velex P. A note on flow regimes and churning loss modeling. Journal of Mechanical Design 2011;133(12):121009, http://dx.doi.org/10.1115/1.4005330.
[15] Attila C, Kozma M. Influence of the oil churning, the bearing and the tooth friction losses on the efficiency of planetary gears. Journal of Mechanical Engineering 2010;56:245–52.
[16] Biboulet N, Houpert L. Hydrodynamic force and moment in pure rolling lubricated contacts. Part 1: line contacts. Proceedings of the IMechE. Part J: Journal of Engineering Tribology 2010;224(8):765–75.
[17] Morales-Espejel G. Using a friction model as an engineering tool. Evolution SKF 2006;2:27–30.
[18] Harris T, Rumbarger J, Butterfield C. Wind turbine design guideline dg03: yaw and pitch rolling bearing life. Technical report. National Renewable Energy Laboratory; December 2009.
[19] Gold PW, Schmidt A, Dicke, Loos J, Assmann C. Viscosity–pressure–temperature behavior of mineral and synthetic oils. Journal of Synthetic Lubrication 2001;18(1):51–79.
[20] Cousseau T, Graça B, Campos A, Seabra J. Experimental measuring procedure for the friction torque in rolling bearings. Lubrication Science 2010;22(April (4)):133–47.
[21] Hamrock BJ, Dowson D. Ball bearing lubrication. John Wiley & Sons; 1981. p. 386.
[22] Brandão JA, Meheux M, Seabra JHO, Ville F, Castro MJD. Traction curves and rheological parameters of fully formulated gear oils. Proceedings of the Institution of Mechanical Engineers, Part J: Journal of Engineering Tribology 225:577–93. http://dx.doi.org/10.1177/1350650111405111, In press.
[23] Astm d341-09. Standard practice for viscosity–temperature charts for liquid petroleum products.